

Manuscript Number:

Title: Synthesis and characterization of Fe₃O₄@Cs@Ag nanocomposite and its use in the production of magnetic and antibacterial nanofibrous membranes

Article Type: Full Length Article

Keywords: Fe₃O₄@Cs@Ag, nanofiber, magnetic property, antibacterial activity

Corresponding Author: Dr. Derman Vatansever Bayramol, Ph.D.

Corresponding Author's Institution:

First Author: Aylin Yıldız

Order of Authors: Aylin Yıldız; Derman Vatansever Bayramol, Ph.D.; Rıza Atav; Ahmet Özgür Ağırhan; Uğur Ergünay; Mine Kurç; Ravi L Hadimani; Carl Mayer

Abstract: Electrospinning is a promising technique to produce polymeric as well as metal oxide nanofibers in diverse domains. In this work, different weight ratios (5%, 7.5% and 10%) of Fe₃O₄@Cs@Ag magnetic nanoparticles were added in PVP (polyvinylpyrrolidone) polymer and fabricated via electrospinning method to produce magnetic nanofibers (MNFs). Structural, magnetic, morphological, spectroscopic and thermal properties of produced nanofibers were characterized. Furthermore, antibacterial effects of Fe₃O₄@Cs@Ag nanofibrous membrane was investigated. Obtained SEM images showed that produced nanofibers were uniform and defect free. Moreover, crystallinity and magnetic moment of fibers was tested by using X-ray diffraction and a vibrating sample magnetometer. The results showed that produced nanofibrous membranes exhibited good antibacterial activity versus *Staphylococcus aureus*, *Bacillus subtilis*, *Enterococcus faecalis*, *Escherichia coli*, *Proteus mirabilis* and *Pseudomonas aeruginosa*.

Suggested Reviewers: Joao S Amaral
University of Aveiro
jamaral@ua.pt
An expert on materials science and nanomaterials

Mattia Butta
Czech Technical University
buttamat@fel.cvut.cz
An expert on magnetic materials

İbrahim Bahtiyari
Erciyes University
bahtiyari@erciyes.edu.tr
An expert on antibacterial materials

18.02.2020

Dear Editor,

Please find enclosed our manuscript entitled “**Synthesis and characterization of Fe₃O₄@Cs@Ag nanocomposite and its use in the production of magnetic and antibacterial nanofibrous membranes**” for consideration to be published as an article in Applied Surface Science.

We here in confirm that the present manuscript and its contents have not been published previously in some other forms or by any other authors and are not under consideration for publication in another journal at the time of submission.

Thank you very much for your consideration.

Yours Sincerely,

Assoc. Prof. Dr. Derman VATANSEVER BAYRAMOL,

Tekirdağ Namık Kemal University, Faculty of Engineering, Department of Textile Engineering

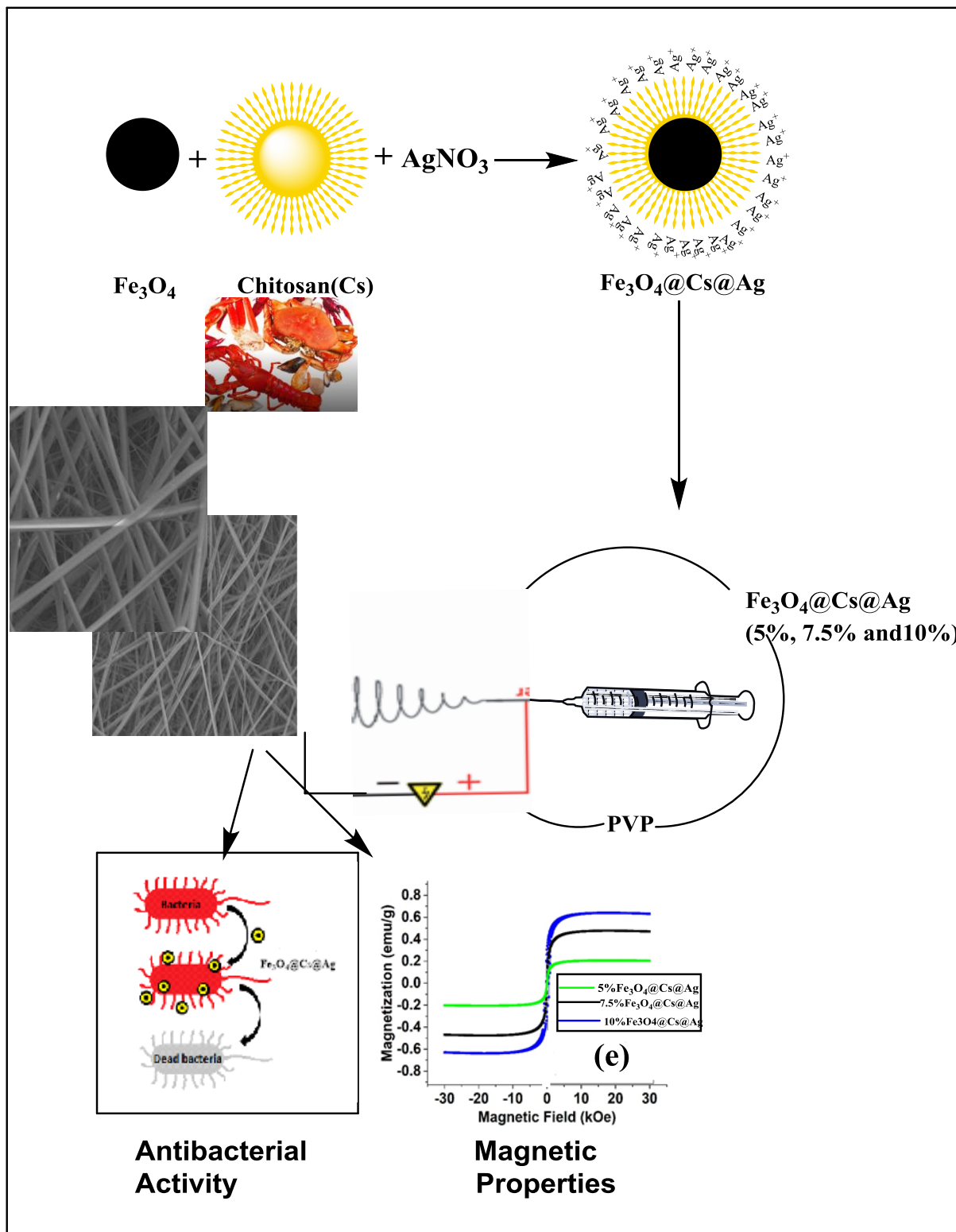
Silahtarağa Mah. Üniversite 1. Sok. No:13, 59860, Corlu/Tekirdag, TURKEY

Phone: +90(282)250 2415

E-mail: dermanvs@gmail.com

Research Highlights

- $\text{Fe}_3\text{O}_4@\text{Cs}@\text{Ag}$ magnetic nanocomposite (MNC) were successfully prepared by simple reflux method.
- $\text{Fe}_3\text{O}_4@\text{Cs}@\text{Ag}$ containing nanofibers were successfully produced by an electrospinning unit.
- The characterization of obtained nanofibers were performed
- Antibacterial and magnetic properties of produced nanofibers were investigated.



Synthesis and characterization of Fe₃O₄@Cs@Ag

nanocomposite and its use in the production of magnetic and antibacterial nanofibrous membranes

Aylin YILDIZ¹, Derman VATANSEVER BAYRAMOL^{1,*}, Rıza ATAV¹, A. Özgür AĞIRGAN¹, Uğur ERGÜNAY¹, Mine Aydın KURÇ², R. L. HADIMANI^{3,4}, Carl MAYER⁵

*corresponding author: dermanvs@gmail.com

¹Faculty of Engineering, Department of Textile Engineering, Tekirdağ Namık Kemal University, Çorlu, Turkey

²School of Medicine, Department of Microbiology, Tekirdağ Namık Kemal University, Tekirdağ, Turkey

³Department of Mechanical and Nuclear Engineering, Virginia Commonwealth University, Richmond VA 23284, USA

⁴Department of Biomedical Engineering, Virginia Commonwealth University, Richmond VA 23284, USA

⁵Nano Characterization Center, Virginia Commonwealth University, Richmond VA 23284, USA

Abstract

Electrospinning is a promising technique to produce polymeric as well as metal oxide nanofibers in diverse domains. In this work, different weight ratios (5%, 7.5% and 10%) of Fe₃O₄@Cs@Ag magnetic nanoparticles were added in PVP (polyvinylpyrrolidone) polymer and fabricated via electrospinning method to produce magnetic nanofibers (MNFs). Structural, magnetic, morphological, spectroscopic and thermal properties of produced nanofibers were characterized. Furthermore, antibacterial effects of Fe₃O₄@Cs@Ag nanofibrous membrane was investigated. Obtained SEM images showed that produced nanofibers were uniform and defect free. Moreover, crystallinity and magnetic moment of

fibers was tested by using X-ray diffraction and a vibrating sample magnetometer. The results showed that produced nanofibrous membranes exhibited good antibacterial activity versus *Staphylococcus aureus*, *Bacillus subtilis*, *Enterococcus faecalis*, *Escherichia coli*, *Proteus mirabilis* and *Pseudomonas aeruginosa*.

Keywords: Fe₃O₄@Cs@Ag, nanofiber, magnetic property, antibacterial activity

1. Introduction

Electrospinning, is a fiber production technique used to produce fine-fibers with a diameter in nano scale via electrostatic force created between two electrodes. This fiber production technique has a potential to be used in diverse fields therefore, lately, a significant number of studies have been concentrated on nanoscale fiber production [1]. To produce nanofiber structures via electrostatic force, both natural and synthetic polymers can be used as raw materials polymer solution [2]. The advantages of using electrospinning technique are porosity, ductility, high specific surface area, fine diameter of fibers ranges from several nanometers to several microns, controllability and design of the fiber formation [3]. Therefore, it can be considered as a versatile technique for nano-scale fiber composites and porous structures. Electrospun nanofiber structures have a wide range of applications including but limited to filtration, material reinforcement, energy storage, wound dressings and so on. [4-6].

The interest in developing new nanomaterials has aroused recently due to its wide range of potential applications in multiple fields [7-10]. Due to magnetic and optical properties, magnetic nanomaterials are good candidates for different research areas and multidisciplinary studies. A significant number of magnetic nanoparticles are synthesized however, Fe₃O₄ is the most widely studied one due to its properties such as optical, electrical, spin dependent

transport, super-paramagnetism and low toxicity [11, 12]. Furthermore, Fe₃O₄ can be considered as environmental friendly and it is low in price.

Unique properties of Fe₃O₄ attracted great attention in various applications, such as magnetic recording media [13], drug delivery agents [14] and adsorbents [15, 16]. Biotechnology/biomedicine, medical diagnosis, electrochemical and bioelectrochemical sensing, environmental remediation, catalysis, electrodes for supercapacitors and lithium ion batteries, data storage, magnetic fluids recording, photo catalysis, microwave absorption, material sciences, magnetic resonance imaging are some of the potential applications for Fe₃O₄ and its nanocomposites [17-24]. Lately studies in the literature have focused on the use of magnetic nanoparticles as carriers of drug or gene delivery and as contrast agents for magnetic resonance imaging biomolecules separation [25].

Chitosan is an aminopolysaccharide biopolymer derived by N-deacetylation of chitin, whose structure may be regarded as cellulose, but chitin has acetamide groups (-NHCOCH₃) instead of the hydroxyl [-OH] at the C2-portion [26]. It is a linear polycation with high charge density, reactive hydroxyl and amino groups as well as extensive hydrogen bonding. Its biocompatibility, physical stability and processability make chitosan important for a number of applications [27]. Chitin is characterized as white, non-elastic, hard, nitrogenous polysaccharides that have been estimated to be synthesized in approximately one billion tons annually [28,29]. Chitosan is derived from chitin, which can be found in nature, as the structural component of crabs, shrimps, lobsters, and insects, in algae, and some fungal cell walls [30,31]. Chitosan is composed of β (1→4)-linked 2-acetamido-2-deoxy-β-D-glucose (N-acetylglucosamine). Chitosan can also be obtained from dimorphic fungi, such as *Mucor rouxii*, by the action of the deacetylase enzyme on chitin [32-34]. Due to its high biodegradability, nontoxicity and antimicrobial properties, a significant number of

applications of chitosan is to use it as an antimicrobial agent either alone or blended with other natural polymers [35]. Important properties of chitosan and its oligosaccharides include: antifungal and antibacterial [36, 37]; anti-inflammatory [38]; antitumour [38]; neuroprotective [40].

Textile fabrics have a potential to be used in many applications due to their versatility and ease to combine with composite materials [41]. Production of technical and functional textiles can be considered as important milestones in textile industry. One of the most desired functionality in textiles is being antibacterial for not only in medical applications but also in daily life. Therefore, production of antibacterial textiles has increased for a number of application areas, including but not limited to hygienic and medical applications [42]. One of the material which is desirable for industrial applications, where good conductivity, chemical stability, and catalytic and antibacterial activity required, is colloidal silver [43]. Silver has been a potential material for medical applications since ancient times due to antibacterial, antifungal and antiviral effects of silver ions. [44-46]. A complex compound of silver was previously synthesised and used as an antibacterial agent in finishing process of a cotton fabric [47]. Using silver ions in a complex compound offers some advantages, such as not getting into the skin when contacted that makes it possible to be used as a new antibacterial agent in textiles [47].

In this study, it was aimed to produce nanowebs including silver in complex form and having antibacterial functionality. To achieve higher antimicrobial effect, a nanocomposite material consisting of Fe_3O_4 , chitosan (Cs) and Ag was synthesised and characterised. Synthesised $\text{Fe}_3\text{O}_4@\text{Cs}@Ag$ nanocomposite was added into polyvinylpyrrolidone (PVP) polymer solution, and produced as a nanoweb via electrospinning device. Then the antibacterial activity of produced $\text{Fe}_3\text{O}_4@\text{Cs}@Ag$ magnetic nanofibers (MNFs) was investigated.

2. Experimental

2.1. Chemicals and instrumentations

FeCl₃.6H₂O, FeCl₂.4H₂O, AgNO₃, NaBH₄, NH₃ and DMSO (Dimethyl sulfoxide) were obtained from Merck (Darmstadt, Germany). High purity chitosan (C₆H₁₂NO₄, Mv 50,000-190,000), polyvinylpyrrolidone (C₆H₉NO)_x, M_w=1.300.000), N,N-dimethylformamide (DMF) and ethanol were purchased from Aldrich and used without further purification. DMEM (Dulbecco's modified Eagle's high glucose medium) and Fetal bovine serum (FBS) were obtained from Capricorn (Capricorn Scientific, Ebsdorfergrund, Germany), while MTT [3-(4 5-dimethylthiazol-2-yl)-2 5-diphenyltetrazolium bromide] was purchased from Serva (Heidelberg, Germany). Nutrient broth and Mueller Hinton (MH) agar were obtained from Difco (Difco, Detroit, USA).

Produced nanocomposites were analysed via a BRUKER VERTEX 70 ATR model Fourier alternating infrared spectrometer (FT-IR-ATR) in transmission mode over the range of 400-4000 cm⁻¹. For obtaining information on crystalline structure and surface morphology of produced materials, PANalytical Empyrean brand X-ray diffraction (XRD) equipment and Quanta FEG 250 model Scanning Electron Microscope (SEM) (FEI, Netherland) were used, respectively.

Magnetic measurements of samples were carried out in Quantum Design's Dynacool superconducting magnetometer that has a field range of -9 T to +9T and a temperature range of 1.9K to 1000K. A Perkin Elmer Instruments brand DSC 4000 model thermogravimetric analyser was used to determine the thermal stability of the materials. For the thermogravimetric analyse, 6 mg of each sample was heated with a heating rate of 10°C/min under nitrogen atmosphere and the results were recorded. Production of nanowebs were

carried out via Inovensa, Inc. brand single-needle electrospinning device, which allows both horizontal and vertical production.

2.2. Preparation of Fe₃O₄@Cs@Ag nanocomposite

A study in the literature was followed for the preparation of Fe₃O₄@Cs@Ag nanocomposite [48]. FeCl₃.2H₂O and FeCl₂.4H₂O salts with a molar ratio of 2:1, and 2 g of chitosan (C₆H₁₂NO₄, Mv 600,000-800,000) were placed in a three-neck flask to obtain Fe₃O₄@Cs. After a homogeneous solution was obtained by stirring at 40°C for 15 min, the pH of the solution was increased to pH ~11-12 by adding NH₃ drop wise. Then obtained black material was put into a reflux, and continuously stirred at 80°C for 2 h in the presence of argon gas. Magnetic decantation method was used to separate Fe₃O₄@Cs from the aqueous solution. Separated Fe₃O₄@Cs was then washed with distilled water several times and dried in the oven at 80°C for 4 h. Obtained Fe₃O₄@Cs was sonicated in 100 mL of deionized water for an hour. After addition of 0.2 mmol/L of AgNO₃ solution in to the mixture, a further ultrasonication was applied for 2 h followed by rapid edition of 0.6 g of NaBH₄. The whole mixture was vigorously stirred for 2 h to allow the reaction. The separation of final nanocomposite (Fe₃O₄@Cs@Ag) was done magnetically. To eliminate any impurities, obtained Fe₃O₄@Cs@Ag was washed with deionized water for several times.

2.3. Production of nanofibrous membranes containing Fe₃O₄@Cs@Ag

Polymer solution, consisting of PVP and absolute ethanol with a ratio of 18% w/v was prepared while three different weight ratios (5%, 7.5% and 10%) of Fe₃O₄@Cs@Ag were homogenously dispersed in DMF (10 mL). These two mixtures were put together and stirred vigorously at 50°C for 6 h to prepare the electrospinning solution. Prepared solution was used in electrospinning device via a 10 mL syringe and a syringe pump. The inner diameter of the

needle was 0.7 mm. Pretrials were done to determine the optimum electrospinning parameters for this particular study. The optimum parameters were found to be 0,5 mLh⁻¹ feeding rate, 17.5 kV high voltage, and 15 cm distance between the needle tip and the collector.

2.4. Determination of antibacterial activity

In our study, antibacterial activity of Fe₃O₄@Cs@Ag nanofiber was determined by using disk diffusion method. *Staphylococcus aureus* (ATCC 29213), *Bacillus subtilis* (NRRL NRS-744), *Enterococcus faecalis* (ATCC 29212), *Escherichia coli* (ATCC 25922), *Proteus mirabilis* (ATCC 12453) and *Pseudomonas aeruginosa* (ATCC 27853) were used as test microorganisms in this study. Bacteria strains were inoculated to nutrient agar and were then activated by incubating at 37°C for 16-24 hours. After incubation, bacteria density was adjusted to 0.5 MacFarland at Mueller Hinton Broth for all microorganisms and then, Mueller Hinton agar were inoculated with a density-adjusted bacterial suspension. Fe₃O₄@Cs@Ag composite in three different concentrations (I: 5%, II: 7.5%, III: 10%) were tested for antibacterial activity. In addition, DMF solution were used as a negative control in the synthesis of the nanofibers and gentamicin disk were also used as a positive control. 5 µl of the prepared test samples (I, II, III and DMF) were impregnated onto sterilised discs prepared by cutting 5 mm pieces from Whatman Filter paper. Prepared samples were placed on plates that were then incubated at a temperature of 37±2°C for 24 hours. Inhibition zone diameters (millimeter) were measured at the end of incubation. Each test was performed three times.

3. Results and Discussion

3.1. Characterization of magnetic nanofibers containing Fe₃O₄@Cs@Ag

FTIR spectra of the pure chitosan, Fe₃O₄@Cs and Fe₃O₄@Cs@Ag given in Fig. 1 confirm that the syntheses of nanoparticles were successful. Peaks seen at 546 cm⁻¹ and 564 cm⁻¹

present the stretching vibrations of Fe-O bond in $\text{Fe}_3\text{O}_4@\text{Cs}$ and $\text{Fe}_3\text{O}_4@\text{Cs}@Ag$ nanocomposites [24]. O-H stretching (ν) vibrations of the water molecules adsorbed on the nanocomposite was seen as a very broad band centered at 3300 cm^{-1} [49]. The N-H vibration peaks for chitosan, $\text{Fe}_3\text{O}_4@\text{Cs}$, $\text{Fe}_3\text{O}_4@\text{Cs}@Ag$ are seen at 1645 cm^{-1} , 1632 cm^{-1} , 1621 cm^{-1} , respectively. Additionally, the C-N vibrations of amino groups are at 1416 cm^{-1} (chitosan), 1409 cm^{-1} ($\text{Fe}_3\text{O}_4@\text{Cs}$), 1355 cm^{-1} ($\text{Fe}_3\text{O}_4@\text{Cs}@Ag$), and the C-O bonds in the ether groups are at 1023 cm^{-1} , 903 cm^{-1} ($\text{Fe}_3\text{O}_4@\text{Cs}$) and 860 cm^{-1} ($\text{Fe}_3\text{O}_4@\text{Cs}@Ag$) [49]. Therefore, it is possible to say that a successful attachment of chitosan to the surface of the Fe_3O_4 nanoparticles was achieved with respect to FT-IR results.

$\text{Fe}_3\text{O}_4@\text{Cs}@Ag$ MNFs containing 5%, 7.5% and 10% of $\text{Fe}_3\text{O}_4@\text{Cs}@Ag$ were also studied under FT-IR for their surface chemistry. The stretching vibrations of Fe-O bond were seen in Figure 1 as a broad peak centered at $\sim 550\text{ cm}^{-1}$ when transmission spectra of $\text{Fe}_3\text{O}_4@\text{Cs}@Ag$ and magnetic nanofibers were studied. The peak seen at $\sim 1620\text{ cm}^{-1}$ of the spectrum of $\text{Fe}_3\text{O}_4@\text{Cs}@Ag$ MNFs was attributed to stretching vibrations of -COO groups while the stretching bands at ~ 1360 , $\sim 2900\text{ cm}^{-1}$ detected in the spectrum were attributed to -CH₂, -CH₃ species, respectively [49]. Therefore, it is possible to claim that obtained nanofibers contain magnetic particles of $\text{Fe}_3\text{O}_4@\text{Cs}@Ag$ with regard to the transmission spectrums obtained from FT-IR. The crystal structures and phase investigation of $\text{Fe}_3\text{O}_4@\text{Cs}@Ag$ MNFs (5%, 7.5% and 10%) were performed, and the patterns obtained from XRD are shown in Figure 2b. The existence of both Fe_3O_4 ((220), (311)) (JCPDSNo.75-0033) and Ag (111) (JCPDSNo.87-0720) was confirmed in XRD patterns of MNFs containing 7.5% and 10% of $\text{Fe}_3\text{O}_4@\text{Cs}@Ag$ [50, 51]. However, these peaks were not observed in the XRD pattern of MNFs containing 5% $\text{Fe}_3\text{O}_4@\text{Cs}@Ag$.

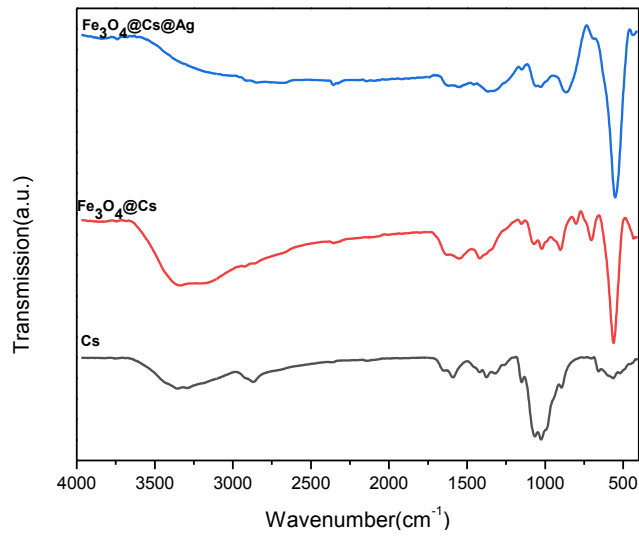


Figure 1: FT-IR spectra of $\text{Fe}_3\text{O}_4@\text{Cs}@\text{Ag}$ nanocomposite

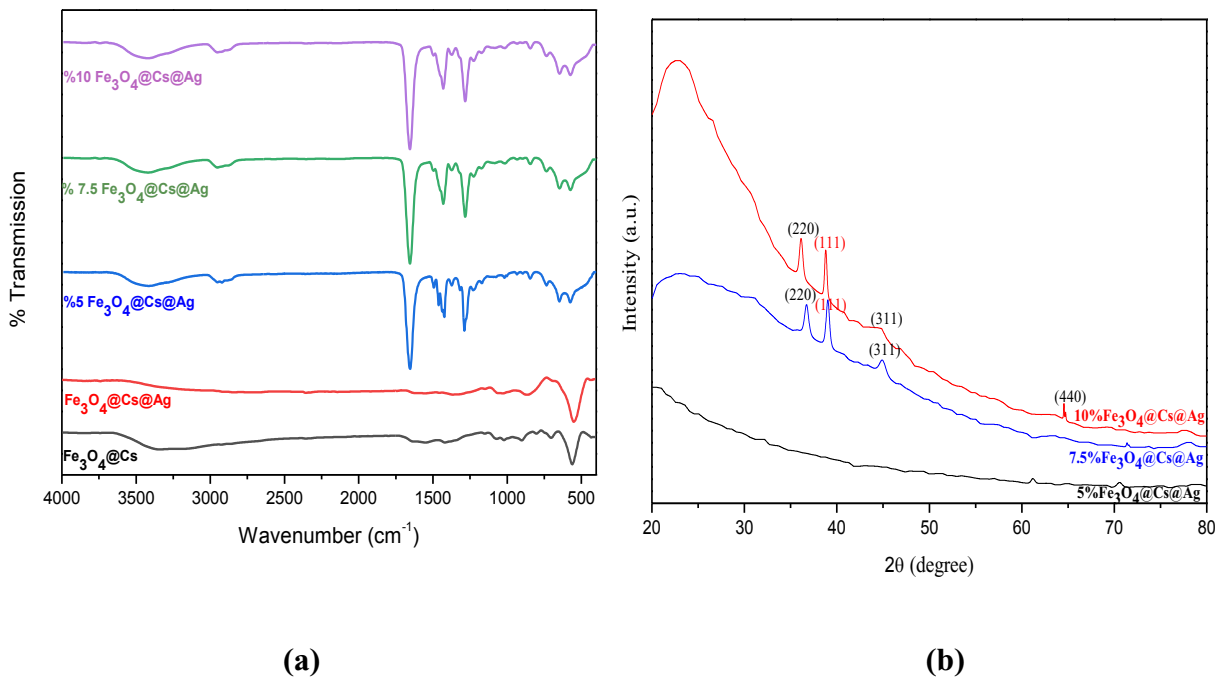


Figure 2. (a) FT-IR spectra of $\text{Fe}_3\text{O}_4@\text{Cs}$ nanocomposite, $\text{Fe}_3\text{O}_4@\text{Cs}@\text{Ag}$ magnetic nanocomposite and $\text{Fe}_3\text{O}_4@\text{Cs}@\text{Ag}$ MNFs (5%, 7.5% and 10%); (b) XRD patterns of $\text{Fe}_3\text{O}_4@\text{Cs}@\text{Ag}$ magnetic nanofibers (5%, 7.5% and 10 %)

TGA thermograms of the $\text{Fe}_3\text{O}_4@\text{Cs}$ nanocomposite, $\text{Fe}_3\text{O}_4@\text{Cs}@Ag$ magnetic nanocomposite and $\text{Fe}_3\text{O}_4@\text{Cs}@Ag$ MNFs (5%, 7.5% and 10%) are given in Figure 3. Weight loss of 10% detected between 20°C and 150°C can be a result of solvent and/or water evaporation. However, in case of $\text{Fe}_3\text{O}_4@\text{Cs}$ and $\text{Fe}_3\text{O}_4@\text{Cs}@Ag$ nanocomposites weight loss occurred between 250°C and 500°C are connected with the decomposition of chitosan. As $\text{Fe}_3\text{O}_4@\text{Cs}@Ag$ nanocomposite contain lower chitosan amount in weight (%), weight loss was not as sharp as $\text{Fe}_3\text{O}_4@\text{Cs}$. On the other hand, the evident peak observed in TGA thermograms of the $\text{Fe}_3\text{O}_4@\text{Cs}@Ag$ MNFs between 450 and 500°C are related to the decaying of chitosan and ignition of PVP.

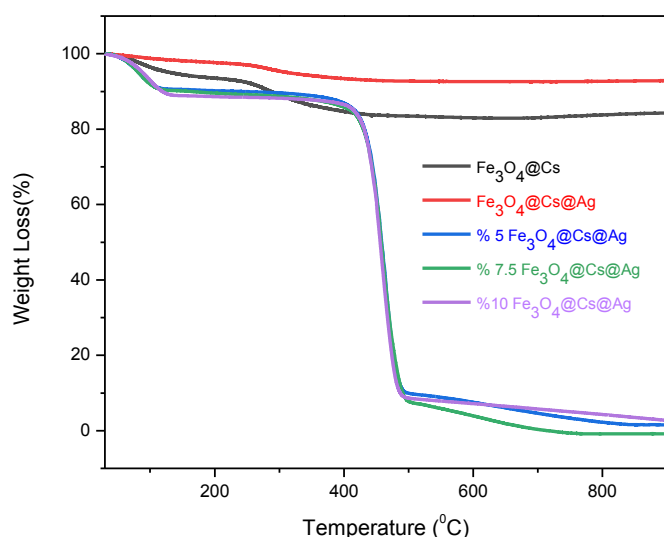
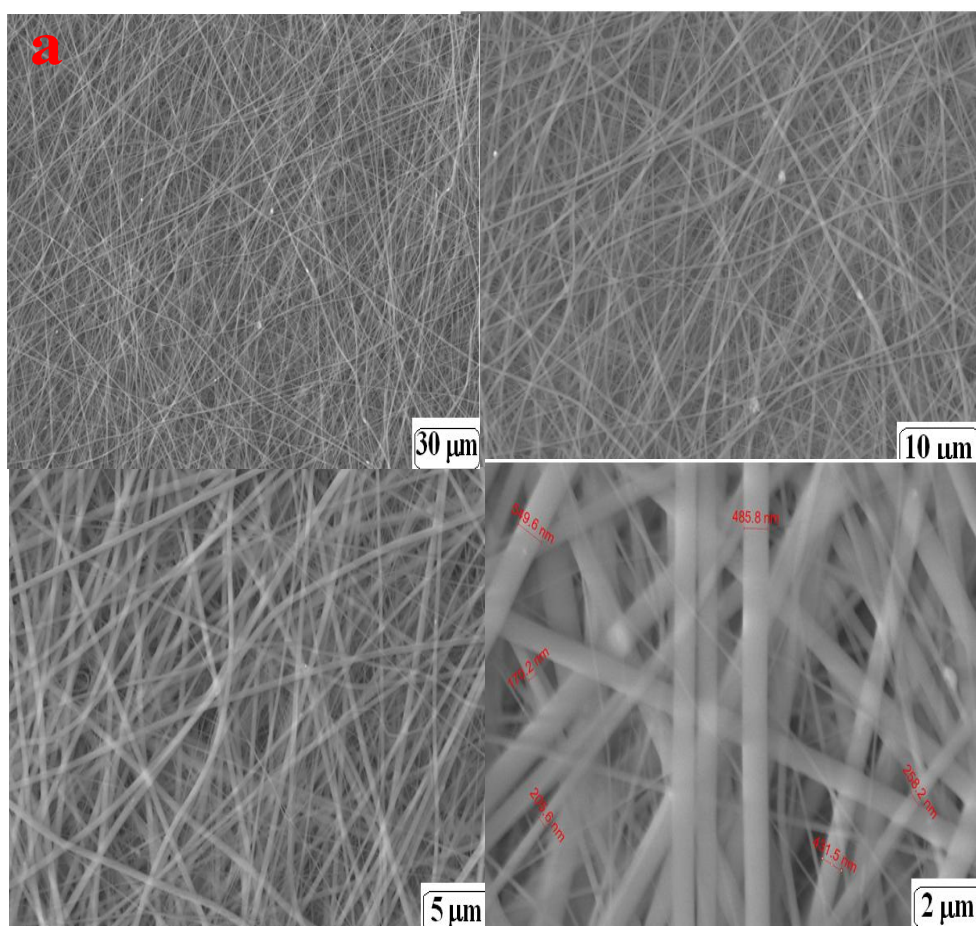


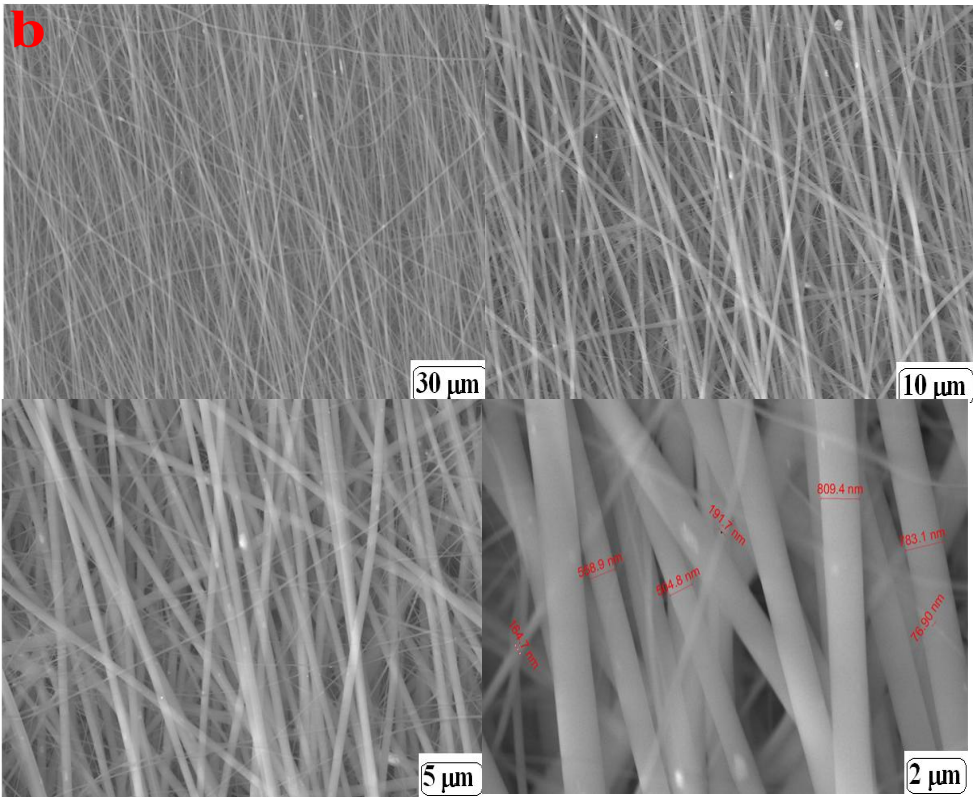
Figure 4. TGA thermograms of $\text{Fe}_3\text{O}_4@\text{Cs}$ nanocomposite, $\text{Fe}_3\text{O}_4@\text{Cs}@Ag$ magnetic nanocomposite and $\text{Fe}_3\text{O}_4@\text{Cs}@Ag$ MNFs (5%, 7.5% and 10%)

The surface morphology of $\text{Fe}_3\text{O}_4@\text{Cs}@Ag/\text{PVP}$ MNF nanowebs containing 5%, 7.5% and 10% $\text{Fe}_3\text{O}_4@\text{Cs}@Ag$ can be seen from the SEM images given in Figure 4. It can be said that successful and bead free magnetic nanofiber production was confirmed by

the SEM images. It should be noted that the distribution of fiber diameter was between 200 nm and 500 nm.

The chemical composition of $\text{Fe}_3\text{O}_4@\text{Cs}@\text{Ag}$ MNFs were determined with a quantitative elemental analysis from EDX measurements. Obtained EDX spectra of $\text{Fe}_3\text{O}_4@\text{Cs}@\text{Ag}$ MNFs are shown in Figure 5. An increase in the amount of Ag and Fe was detected in EDX graphs due to the increase in $\text{Fe}_3\text{O}_4@\text{Cs}@\text{Ag}$ in electrospinning solution. This confirms the successful electrospinning process and magnetic nanofiber production.





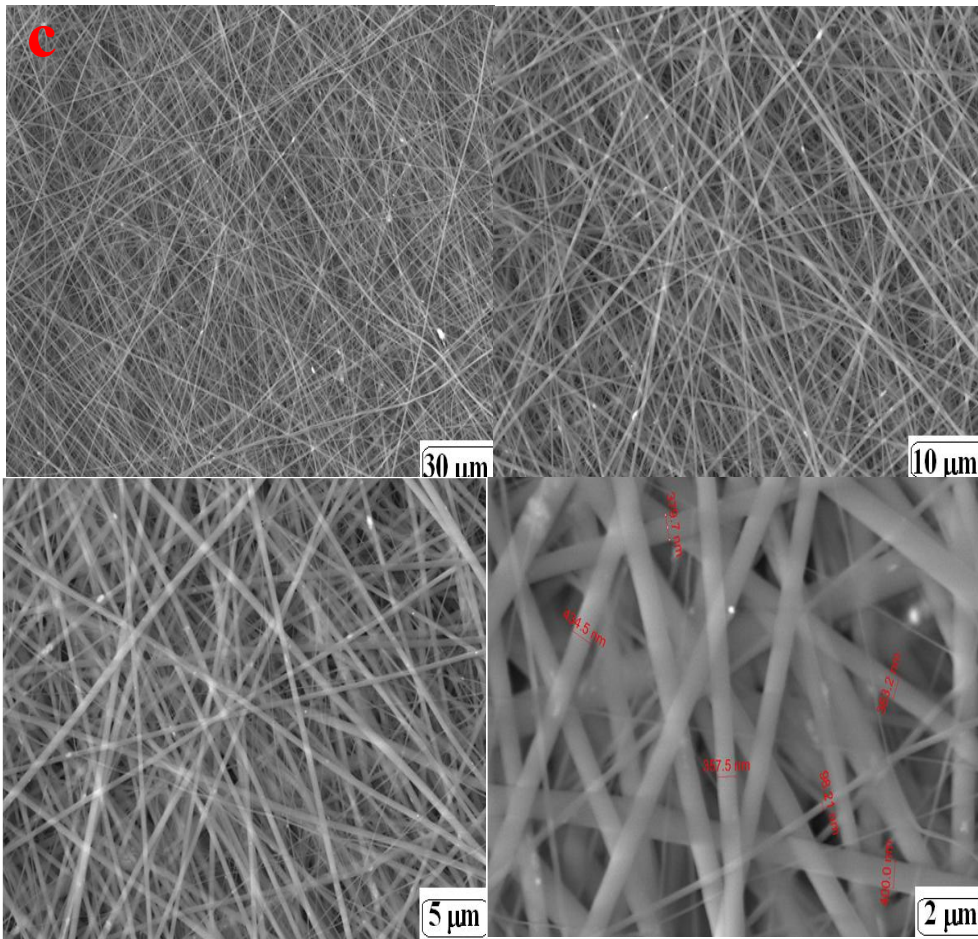


Figure 5. SEM images of magnetic nanofibers containing (a) 5%; (b) 7.5% and (c) 10% $\text{Fe}_3\text{O}_4@\text{Cs}@\text{Ag}$ in the fiber structure

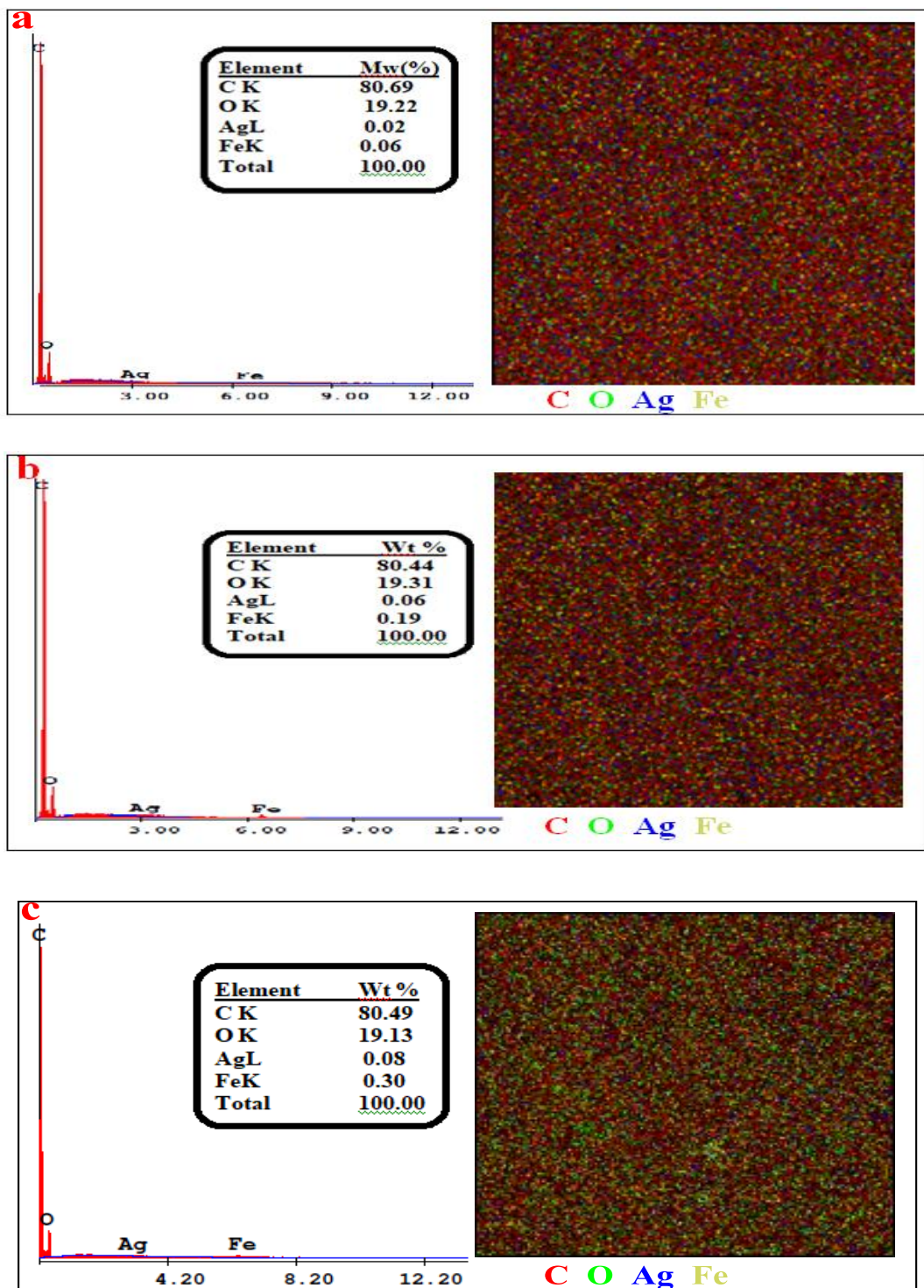


Figure 6. EDX spectra of magnetic nanofibers containing (a) 5%; (b) 7.5% and (c) 10% of $\text{Fe}_3\text{O}_4@\text{Cs}@\text{Ag}$ in the fiber structure

Magnetic measurements of samples were also carried out. Figure 7 (a)-(c) show magnetization as a function of magnetic field for 5%, 7.5% and 10% Fe₃O₄@Cs@Ag measured at a temperature of 300 K. The inset figures in Figure 7 a, b, c show the magnified portion of the hysteresis graphs highlighting small coercivity. 5%, 7.5% and 10% Fe₃O₄@Cs@Ag have a coercivities of 20 Oe, 20 Oe and 25 Oe respectively. Figure 7 (d) shows hysteresis graphs of all 3 samples between magnetic field range of +3T to -3T (+30 kOe to -30 kOe) at an interval of 100 Oe. It can be noted that hysteresis graphs do not saturate even at an applied magnetic field of 30 kOe. This is because of the paramagnetic nature of PVP in the samples. The paramagnetic fraction of the sample contributed by PVP was deducted by first calculating the slope of the magnetic curve above 1 T (10 kOe) magnetic field and subtracting it in the original hysteresis graphs. The saturation field of 1 T (10 kOe) was chosen based on the prior literature on Fe₃O₄ [52-55]. Figure 7 (e) shows hysteresis graphs of 5%, 7.5% and 10% Fe₃O₄@Cs@Ag after removing the paramagnetic contribution from the original hysteresis graphs. The coercivity and the remanence magnetization of the hysteresis graph didn't change significantly after the removal of paramagnetic contribution of PVP.

Saturation magnetization of high purity Fe₃O₄ nanoparticles range from 80 emu/g to 100 emu/g based on the method of preparation [52-56]. The saturation magnetic field of pure Fe₃O₄ nanoparticles is reported to be below 10kOe [52, 54]. However, the saturation magnetization of composite materials that have magnetic nanoparticles will be significantly smaller due to contribution of mass of non-magnetic constituent of the composite material.

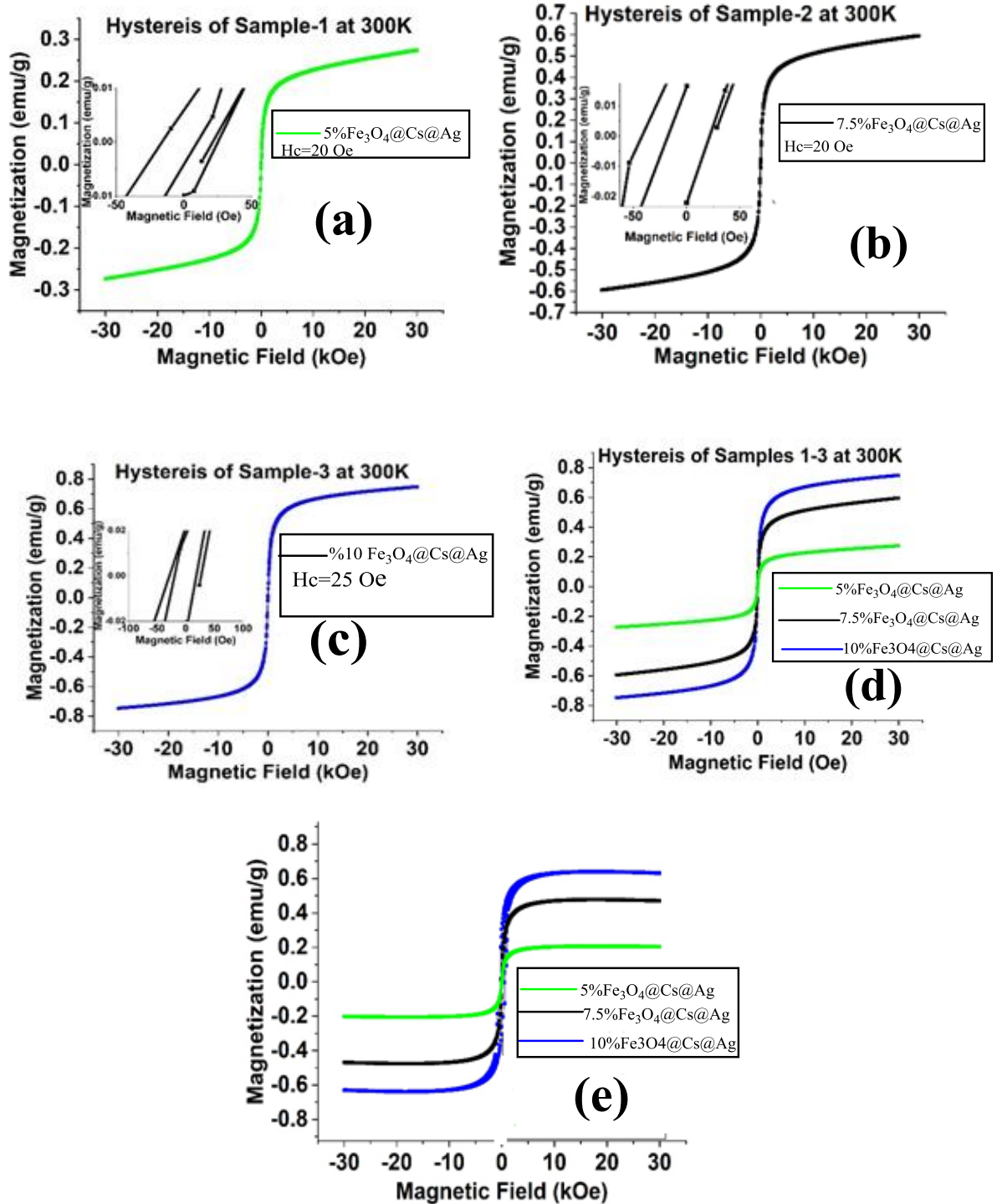


Figure 7 Magnetization as a function of magnetic field measurements at 300 K on (a) sample 1 (b) sample 2 (c) sample 3. Inset of (a), (b) and (c) graphs show coercivity of 20 Oe, 20 Oe and 25 Oe respectively. (d) shows combined hysteresis graphs between 3T (30 kOe) and -3T (30 kOe) and (e) shows hysteresis graph after removal of paramagnetic part of PVP.

It can be attributed that the reduced saturation magnetization detected in the samples could be caused by following circumstances; surface spins canting, which was resulted by competing antiferromagnetic interactions [50], randomly dispersed small particles exhibiting high magneto-crystalline anisotropy caused unsaturation effect [51], spin glass characteristics [52], magnetic inactive layer formation [53] and the disordering cations distribution [54] on the surface of nanoparticles.

Table 1 shows saturation magnetization, remanence magnetization in emu/g, ratio of remanence and saturation magnetization and coercive fields for 5%, 7.5% and 10% Fe₃O₄@Cs@Ag at room temperature. These values are derived from Figure 7. All the three samples show very low coercive fields and low remanence magnetization. The ratio of remanence and saturation magnetization is also significantly below 0.5, indicating that the magnetic nanoparticles are soft ferromagnetic and have uniaxial anisotropy [57].

Table 1. Magnetic properties of 5%, 7.5% and 10% Fe₃O₄@Cs@Ag doped PVP nanofibers

Rate (wt %)	M_s (emu/g)	M_r (emu/g)	M_r/M_s	H_c (Oe)
PVP	51.37	0.35	0.006	4.5
5% Fe₃O₄@Cs@Ag	0.47	0.009	0.019	20
7.5% Fe₃O₄@Cs@Ag	0.20	0.02	0.1	20
10% Fe₃O₄@Cs@Ag	0.63	0.03	0.048	25

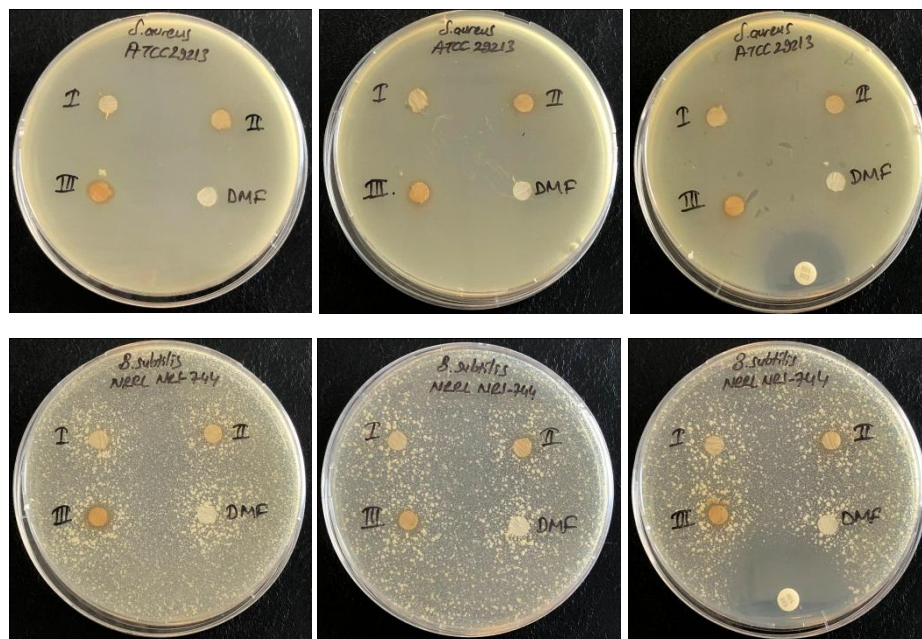
3.2. Determination of antibacterial activity

The antibacterial activities by disk diffusion method of inhibition zones of Fe₃O₄@Cs@Ag magnetic nanofibers were given in Table 2 and Figure 8. As it could be seen from Table 2 the antibacterial activity increased depending on concentration levels.

Table 2. Inhibition zones of Fe₃O₄@Cs@Ag MNFs in mm

	<i>S. aureus</i> ATCC 29213	<i>B. subtilis</i> NRRL NRS-744	<i>E. faecalis</i> ATCC 29212	<i>E. coli</i> ATCC 25922	<i>P. mirabilis</i> ATCC 12453	<i>P. aeruginosa</i> ATCC 27853
I	ND	ND	8.33±0.57	7.33±0.57	7.0±1.0	ND
II	6.66±0.57	ND	8.66±0.57	7.66±0.57	7.33±0.57	6.33±0.57
III	8.0±1.0	6.33±0.57	8.66±0.57	9.0±1.0	8.33±0.57	7.66±0.57
DMF	ND	ND	ND	ND	ND	ND

Values are mean of triplicate readings (mean ± S.D). ND= Not detected



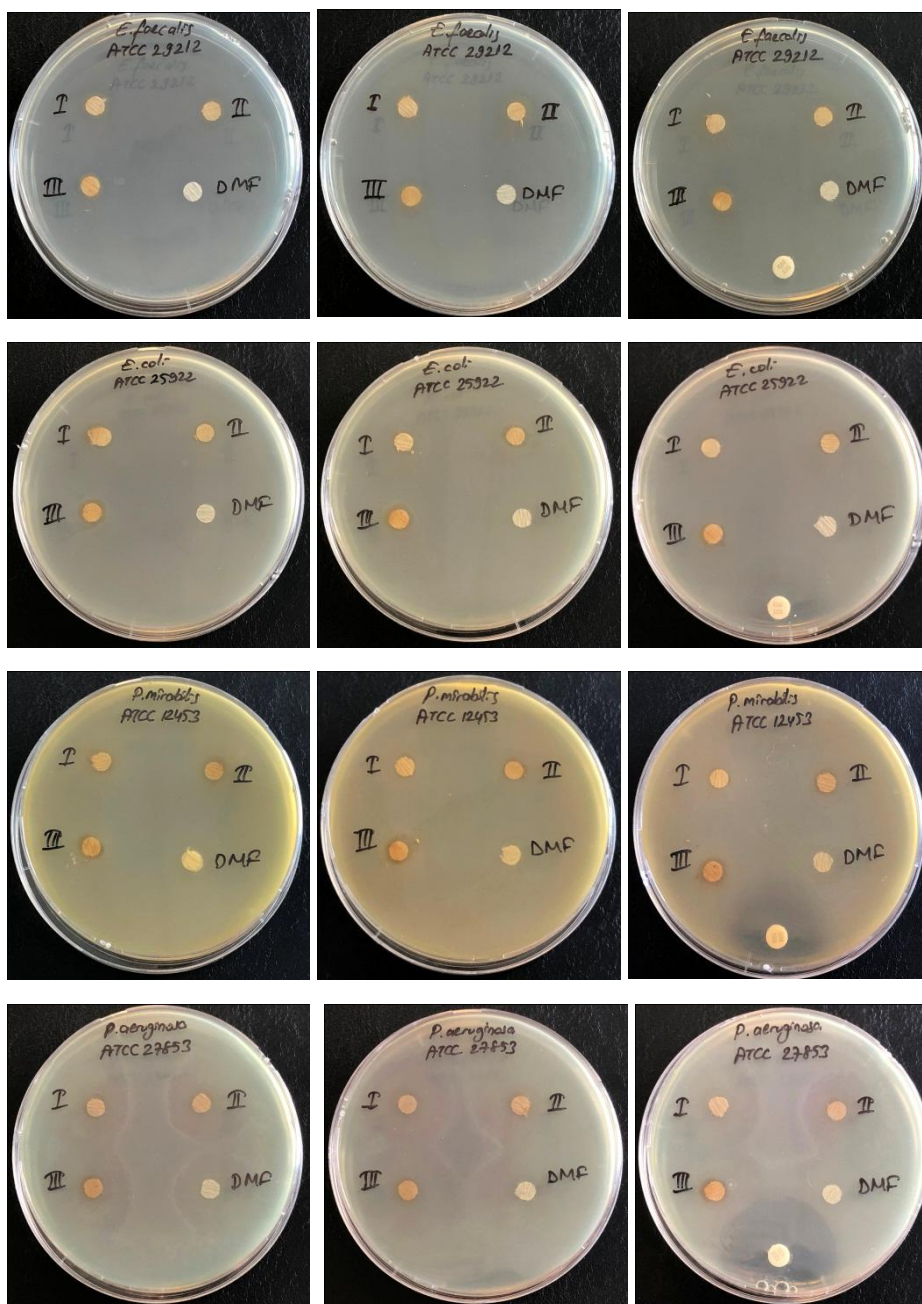


Figure 8. Antibacterial activity of fabricated nanofibers containing 3 different concentrations of $\text{Fe}_3\text{O}_4@\text{Cs}@\text{Ag}$ magnetic nanofibers (5%, 7.5% and 10%) against six different bacteria. DMF and $\text{Fe}_3\text{O}_4@\text{Cs}@\text{Ag}$ solutions used in the preparation of nanofibers are also tested for antibacterial activity as controls.

To evaluate the antibacterial efficiency of $\text{Fe}_3\text{O}_4@\text{Cs}@\text{Ag}$ nanofiber, it had good effect against *S. aureus*, *E. faecalis*, *E. coli*, *P. mirabilis* and *P. aeruginosa*, on the other hand it

showed lower effect against *B. subtilis* than others. The highest antibacterial activities were obtained against *E. faecalis* and *E. coli* among all microorganisms. The highest concentration (III) of Fe₃O₄@Cs@Ag had good antibacterial effect on all microorganisms except *B. subtilis*. When the results were evaluated, the increasing of Fe₃O₄@Cs@Ag nanocomposite concentration was found to be effective in antibacterial activity.

4. Conclusion

Magnetic nanofibers containing 5%, 7.5% and 10% of Fe₃O₄@Cs@Ag were produced via solution electrospinning technique. FT-IR results confirmed the successful MNF production due to clear Fe-O bonds, prove the existence of Fe₃O₄@Cs@Ag in the structure. These results were also supported by the results obtained from XRD. EDX results indicated that produced nanofibers contained both Fe and Ag, and their amount increased with the increase in Fe₃O₄@Cs@Ag concentration in the electrospinning solution. SEM images showed that uniform magnetic nanofibers with a fiber diameter range of 200-400 nm were successfully produced. The results obtained from VSM analysis indicated that produced nanofibers showed soft superparamagnetic (SPM) behavior at room temperature. Furthermore, antibacterial test results of produced Fe₃O₄@Cs@Ag MNFs showed that the concentration of Fe₃O₄@Cs@Ag in nanofibres was an important parameter, and Fe₃O₄@Cs@Ag MNFs can be good candidates to be used in applications where magnetic and antibacterial properties are required.

On the other hand, Fe₃O₄ nanoparticles are good candidates for magnetic attenuation sources in electromagnetic shielding composites due to their excellent magnetic and dielectric properties [54]. Conductive textiles are very promising to be used for electromagnetic shielding issues in the field of industry, military and civil wearable technologies as well as

medicine, telecommunication [42]. There are a number of electromagnetic shielding applications of nonwoven and nonwoven coated fabrics with conductive fibers due to their light-weight, flexibility, versatility and grate blending options [55]. For this reason it is thought that the $\text{Fe}_3\text{O}_4@\text{Cs}@\text{Ag}$ compound could also be used for electromagnetic shielding purposes. However, as thin nanoweb layers are produced in this study, electromagnetic shielding functionality was not searched. Because for obtaining electromagnetic shielding effect, the most important parameter is the weight and thickness of the material. Nevertheless, in further studies it is planned to use this compound in composite structures having both electromagnetic shielding and antibacterial effects.

Acknowledgments

This work was supported in part by Scientific Research Unit of Tekirdağ Namık Kemal University within NKUBAP.06.GA.19.195 coded project. Magnetic Characterization at Virginia Commonwealth University was partially supported by National Science Foundation, Award Number: 1726617.

References

1. T. Amna , M.S. Hassan, H. Van Ba, Electrospun $\text{Fe}_3\text{O}_4/\text{TiO}_2$ hybrid nanofibers and their *in vitro* biocompatibility: Prospective matrix for satellite cell adhesion and cultivation, *Mater. Sci. & Eng. C* 2 (2013) 707-713.
2. N. Bhardwaj, S.C. Kundu, Electrospinning: a fascinating fiber fabrication technique, *Biotechnol. Adv.* 28 (2010) 325–347.
3. A. Baji, Y.W. Mai, S.C. Wong, M. Abtahi, P. Chen, Electrospinning of polymer nanofibers: effects on oriented morphology, structures and tensile properties, *Compos. Sci. & Technol.* 70 (2010) 703–718.
4. J. Aldana, N. Lavelle, Y. Wang, X. Peng, Size-dependent dissociation pH of thiolate ligands from cadmium chalcogenide nanocrystals, *J. Am. Chem. Soc.*, 127 (2005) 2496–2504.

5. S.K. Poznyak, N.P. Osipovich, A. Shavel, D.V. Talapin, M.Y. Gao, A. Eychmuller, et al., Size-dependent electrochemical behavior of thiol-capped CdTe nanocrystals in aqueous solution, *J. Phys. Chem. B* 109 (2005) 1094–1100.
6. S. Thenmozhi, N. Dharmaraj, K. Kadirvelu, H.Y. Kim, Electrospun nanofibers: New generation materials for advanced applications, *Mater. Sci. & Eng. B* 217 (2017) 36–48.
7. P. Chen, H. Li, S. Song, X. Weng, D. He, Y. Zhao, Adsorption of dodecylamine hydrochloride on graphene oxide in water, *Results Phys* (2017) 2281–2288.
8. Á. de J. Ruíz-Baltazar, S.Y. Reyes-López, R. Pérez, Magnetic structures synthesized by controlled oxidative etching: structural characterization and magnetic behavior, *Results Phys* (2017) 1828–1832.
9. A.O. Baskakov, A.Y. Soloveva, Y.V. Ioni, S.S. Starchikov, I.S. Lyubutin, I.I. Khodos, A.S. Avilov, S.P. Gubin, Magnetic and interface properties of the core-shell Fe₃O₄/Au nanocomposites, *Appl Surf Sci* (2017) 638–644.
10. E. Mohammadiyan, H. Ghafuri, A. Kakanejadifard, Synthesis and characterization of a magnetic Fe₃O₄@CeO₂ nanocomposite decorated with Ag nanoparticle and investigation of synergistic effects of Ag on photocatalytic activity, *Optik (Stuttg)* (2018) 39–48.
11. H. Nouredini, X. Gao, R.S. Philkana, *Bioresour. Technol.* 96 (2005) 769–777.
12. A.K. Gupta, M. Gupta, *Biomaterials* 26 (2005) 3995–4021
13. J.H. Lee, Y.M. Huh, Y.W. Jun, J.W. Seo, J.T. Jang, H.T. Song, S. Kim, E.J. Cho, H.G. Yoon, J.S. Suh, J. Cheon, Artificially engineered magnetic nanoparticles for ultrasensitive molecular imaging, *Nat Med* 13 (2007) 95–99.
14. H.E. Ghandoor, H.M. Zidan, M.H. Khalil, M.I.M. Ismail, Synthesis and some physical properties of magnetite (Fe₃O₄) nanoparticles, *Int J Electrochem Sci* 7 (2012) 5734–5745.
15. S. Bao, K. Li, P. Ning, J. Peng, X. Jin, L.H. Tang, Synthesis of amino-functionalization magnetic multi-metal organic framework (Fe₃O₄/MIL-101(A_{10.9}Fe_{0.1})/NH₂) for efficient removal of methyl orange from aqueous solution. *J Taiwan Inst Chem E* 87 (2018) 64–72.
16. K. Kamari, A. Taheri, Preparation and evaluation of magnetic core-shell mesoporous molecularly imprinted polymers for selective adsorption of amitriptyline in biological samples, *Taiwan Inst Chem E* 86 (2018) 230–239.
17. S. Singamaneni, V.N. Bliznyuk, C. Binek, E.Y. Tsymbal, Magnetic nanoparticles: recent advances in synthesis, self-assembly and applications, *J. Mater. Chem.* 21 (2011) 16819–16845.
18. T. Xie, L. Xu, C. Liu, Synthesis and properties of composite magnetic material SrCo_xFe_{12-x}O₁₉ (x= 0-0.3), *Powder Technol.* 232 (2012) 87-92.
19. T. An, J. Chen, X. Nie, G. Li, H. Zhang, X. Liu, H. Zhao, Synthesis of Carbon Nanotube–Anatase TiO₂ Sub-micrometer-sized Sphere Composite Photocatalyst for

- Synergistic Degradation of Gaseous Styrene. *ACS Appl. Mater. & Interfaces* 4 (2012) 5988-5996.
20. H. Teymourian, A. Salimi, S. Khezrian, Fe₃O₄ magnetic nanoparticles/reduced graphene oxide nanosheets as a novel electrochemical and bioelectrochemical sensing platform, *Biosens. Bioelectron* 49 (2013) 1-8.
 21. B. Zhang, Y. Du, P. Zhang, H. Zhao, L. Kang, X. Han, P. Xu, Microwave absorption enhancement of Fe₃O₄/polyaniline core/shell hybrid microspheres with controlled shell thickness, *J. Appl. Sci.* 130 (2013) 1909–1916.
 22. M. Rashad, I. Ibrahim, Structural, microstructure and magnetic properties of strontium hexaferrite particles synthesised by modified coprecipitation method, *Mater. Technol.* 27 (2012) 308-314.
 23. N.A. Frey, S. Peng, K. Cheng, S. Sun, Magnetic nanoparticles: synthesis, functionalization, and applications in bioimaging and magnetic energy storage, *Chem. Society Rev.* 38 (2009) 2532-2542.
 24. Md. Amir, S. Güner, A. Yıldız, A. Baykal, Magneto-optical and catalytic properties of Fe₃O₄@HA@Ag magnetic nanocomposite, *J. of Magnetism & Magn. Mater.* 421 (2017) 462-471.
 25. T.K. Indira, P.K. Lakshmi, Magnetic Nanoparticles: A Review, *Int. J. Pharm. Sci. & Nanotechnol.* 3 (2010) 1035-1042.
 26. S. Suzuki, Biological effects of chitin, chitosan, and their oligosaccharides, *Biotherapy.* 14 (2000) 965–971.
 27. M.N.V. Kumar, A review of chitin and chitosan applications, *Reactive Funct Polym.* 46 (2000) 1–27.
 28. R.A. Muzzarelli, *Chitin*, Pergamon Press (1977) Oxford, UK,
 29. R.A. Muzzarelli, C. Muzzarelli, Chitosan chemistry: Relevance to the biomedical sciences. *Adv Polym Sci.* 186 (2005) 151–209.
 30. R.N. Tharanathan, F.S. Kittur, Chitin – the undisputed biomolecule of great potential, *Crit Rev Food Sci Nutr.* 43 (2003) 61–87. Y. Shigemasa, S. Minami, Applications of chitin and chitosan for biomaterials, *Biotechnol Genet Eng Rev.* 13 (1995) 383–420.
 32. I. Aranaz, M. Mengibar, R. Harris, I. Paños, B. Miralles, N. Acosta, G. Galed, A. Heras, Functional characterization of chitin and chitosan, *Curr Chem Biol.* 3 (2009) 203–230.
 33. S.S. Koide, Chitin-Chitosan: Properties, benefits and risks, *Nutr Res.* 18 (1998) 1091–1101.
 34. M.V. Kumar, S.M. Hudson, Chitosan. In: Wnek GE, Bowlin GL, editors. *Encyclopedia of Biomaterials and Biomedical Engineering*. New York: Marcel Dekker (2004) 310–323.

35. M. Kong, X.G. Chen, K. Wing, H.J. Park, Antimicrobial properties of chitosan and mode of action: a state of the art review, *Int J Food Microbiol.* 144 (2010) 51-63.
36. J.C. Fernandes, F.K. Tavoria, J.C. Soares, O.S. Ramos, M. JoaoMonteiro, M.E. Pintado, F. Xavier Malcata, Antimicrobial effects of chitosans and chitooligosaccharides, upon *Staphylococcus aureus* and *Escherichia coli*, in food model systems, *Food Microbiology* 25 (2008) 922-928.
37. Y. Wang, P. Zhou, J. Yu, X. Pan, P. Wang, W. Lan, S. Tao, Antimicrobial effect of chitooligosaccharides produced by chitosanase from *Pseudomonas CUY8*, *Asia Pacific Journal of Clinical Nutrition*, 16 (2007) 174-177.
38. E.J. Yang, J.G. Kim, J.Y. Kim, S. Kim, N. Lee, C.K. Hyun, Anti-inflammatory effect of chitosan oligosaccharides in RAW 264.7 cells, *Central European Journal of Biology* 5 (2010) 95-102,
39. H. Quan, F. Zhu, X. Han, Z. Xu, Y. Zhao, Z. Miao, Mechanism of anti-angiogenic activities of chitooligosaccharides may be through inhibiting heparanase activity *Medical Hypotheses* 73 (2009) 205-206.
40. R. Pangestuti, S.K. Kim, Neuroprotective properties of chitosan and its derivatives *Marine Drugs* 8 (2010) 2117-2128.
41. R. Abdulla, M.H. Nişancı, A.H. Yüzer, Statistical Analysis of Electromagnetic Shielding Effectiveness of Metal Fiber Blended Fabrics, *Süleyman Demirel University J. Natural & Appl. Sci.* 21 (2017) 711-717.
42. N.O.S. Yurudu, A.K. Erdem, N.Ş. Yurudu, The Evaluation of Antibacterial Activity of Fabrics Impregnated with Dimethyltetradecyl (3-(Trimethoxysilyl) Propyl) Ammonium Chloride, *IUFS J Biol*, 67 (2008) 115-122.
43. V.K. Sharma, R.A. Yngard, Y. Lin, Silver nanoparticles: Green synthesis and their antimicrobial activities, *Adv. in Colloid & Interface Sci.* 145 (2009) 83-96.
44. C.N. Lok, C.M. Ho, R. Chen, Q.Y. He, W.Y. Yu, H. Sun, P.K. Tam, J.F. Chiu, C.M. Chen, Proteomic analysis of the mode of antibacterial action of silver nanoparticles, *J. Proteome. Res.* 5 (2006) 916-924.
45. K.H. Cho, J.E. Park, T. Osaka, S.G. Park, The study of antimicrobial activity and preservative effects of nanosilver ingredient, *Electrochimica Acta* 51 (2005) 956-960.
46. S. Silver, Bacterial silver resistance: molecular biology and uses and misuses of silver compounds, *FEMS Microbiol. Rev.* 27 (2003) 341-353.
47. A. Yildiz, R. Atav, M. Oztas, A.Ö. Ağirgan, D. Gülen, M. Aydin, M. Yeşilyurt, A.D. Kaya, Synthesis of Silver Mono- and Di-Carboxylates and Investigation of their Usage Possibility in Textiles as an Antibacterial Agent, *FIBRES & TEXTILES in Eastern Europe* 23 (2015) 120-125.

48. C. Demir, Fe₃O₄@HA@Ag Sentezi, Yapısının İncelenmesi ve Tekstilde Kullanımı, Tekirdağ Namık Kemal Üniversitesi Fen Bilimleri Enstitüsü Tekstil Mühendisliği Anabilim Dalı, Master Thesis, (2018) Tekirdağ.
49. X.N. Pham, T.P. Nguyen, T.N. Pham, T.T.N. Tran, T.V.T. Tran, Synthesis and characterization of chitosan-coated magnetite nanoparticles and their application in curcumin drug delivery, *Adv. Nat. Sci.: Nanosci. Nanotechnol.* 7 (2016) 045010.
50. Md. Amir, U. Kurtan, A. Baykal, Rapid color degradation of organic dyes by Fe₃O₄@His@Ag recyclable magnetic nanocatalyst, *J. Industrial & Eng. Chem.* 27 (2015) 347-353.
51. U. Kurtan, E. Onuş, Md. Amir, A. Baykal, Fe₃O₄@Hpipe-4@Cu Nanocatalyst for Hydrogenation of Nitro-Aromatics and Azo Dyes, *J. Inorg. & Organomet. Polymers & Mater.* 25 (2015) 1120–1128
52. Y. Wei, B. Han, X. Hu, Y. Lin, X. Wang, X. Deng, Synthesis of Fe₃O₄ nanoparticles and their magnetic properties, in *Procedia Engineering*, 27 (2012) 632–637.
53. M. Anbarasu, M. Anandan, E. Chinnasamy, V. Gopinath, K. Balamurugan, Synthesis and characterization of polyethylene glycol (PEG) coated Fe₃O₄ nanoparticles by chemical co-precipitation method for biomedical applications, *Spectrochim. Acta. A. Mol. Biomol. Spectrosc.* 135 (2015) 536–539.
54. A.K. Singh, O.N. Srivastava, K. Singh, Shape and Size-Dependent Magnetic Properties of Fe₃O₄ Nanoparticles Synthesized Using Piperidine, *Nanoscale Research Letters* 12 (2017) 298.
55. M. Polichetti, M. Modestino, A. Galluzzi, S. Pace, M. Iuliano, P. Ciambelli, M. Sarno, Influence of citric acid and oleic acid coating on the dc magnetic properties of Fe₃O₄ magnetic nanoparticles, *Mater. Today Proc.* (2020) 21-24.
56. C. Nayek, K. Manna, G. Bhattacharjee, P. Murugavel, I. Obaidat, Investigating Size- and Temperature-Dependent Coercivity and Saturation Magnetization in PEG Coated Fe₃O₄ Nanoparticles, *Magnetochemistry* 3 (2017) 19.
57. R.L. Hadimani, Y. Melikhov, M. Han, D.C. Jiles, Magnetocrystalline Anisotropy in Single Crystal Gd₅Si_{2.7}Ge_{1.3}, *IEEE Trans. Magn.* 48 (2012) 3989–3991.

Declaration of interests

The authors declare that they have no known competing financial interests or personal relationships that could have appeared to influence the work reported in this paper.

The authors declare the following financial interests/personal relationships which may be considered as potential competing interests: